

LIGHT-WEIGHT GESTURE SENSING USING FMCW RADAR TIME SERIES DATA

Thomas Stadelmayer^{1,2}, Avik Santra², Robert Weigel¹, Fabian Lurz³

¹Friedrich-Alexander University Erlangen-Nuremberg, ²Infineon Technologies AG,
³Hamburg University of Technology

ABSTRACT

The paper proposes a novel feature extraction approach for FMCW radar systems in the field of short-range gesture sensing. A light-weight processing is proposed which reduces a series of 3D radar data cubes to four 1D time signals containing information about range, azimuth angle, elevation angle and magnitude. The processing is entirely performed in the time domain without using any Fourier transformation and enables the training of a deep neural network directly on the raw time domain data. It is shown experimentally on real world data, that the proposed processing retains the same expressive power as conventional radar processing to range-, Doppler- and angle-spectrograms. Further, the computational complexity is significantly reduced which makes it perfectly suitable for embedded devices. The system is able to recognize ten different gestures with an accuracy of about 95% and is running in real time on a Raspberry Pi 3 B. The delay between end of gesture and prediction is only 150 ms.

Index Terms— Gesture Recognition, Radar Signal Processing, Time Series Classification, FMCW Radar

1. INTRODUCTION

Radar-based gesture recognition systems provide users an intuitive human-machine interface as an alternative to traditional click and touch based interfaces. Gesture recognition has several applications ranging from smart TVs, laptops, smart phones to controlling robotics. Compared to camera-based solution, radar-based gesture solutions are privacy preserving, and can sense minute subtle gesture motions [1, 2].

Multiple papers have already proven the capability of mm-wave radar sensors to recognize various gestures with high accuracy often enabled by interpreting preprocessed data with machine or deep learning [3–8]. The challenges nowadays are to make the systems robust against distortions such as persons walking in the background [9] and to reduce the system complexity in order to enable the market of embedded devices like smart phones [10].

In fact, recent papers are more and more focusing on the implementation on embedded or edge devices. In [11] a 2D CNN optimized for Intel’s Neural Compute Stick 2 is doing the classification based on range spectrograms. However, the

angle of arrival is not estimated and thus only four basic gestures can be recognized. In [12] a feature cube is created by selecting K points from each range-Doppler image (RDI) and estimating their range, Doppler, azimuth angle, elevation angle and magnitude. The feature cubes, which are a compressed representation of the gestures, are interpreted by a 2D CNN. The system is running in real time on a NVIDIA Jetson Nano. The TinyRadarNN presented in [13] and the RadarNet [10] from the ATAP Google team follow a similar principle. The data is preprocessed to RDIs, which are then image wise compressed to a feature vector by a 2D CNN. A series of compressed RDIs is then interpreted by a temporal neural network. In contrast to many other papers the authors of [10] highlight the importance of the phase information and thus are working with complex valued RDIs.

All current solutions using a frequency modulated continuous wave (FMCW) radar rely on RDIs, which are generated by a 2D fast Fourier transformation (FFT) with high computational effort. To the best of our knowledge this is the first work providing an alternative to the dominating FFT based preprocessing for FMCW radars. By minimal processing – without any FFT – a series of 3D radar data cubes is converted into relative range, accumulated azimuth as well as elevation angle and magnitude over slow time. Using real world data we demonstrate the classification performance of a deep neural network trained by our proposed time series data in comparison with conventional range-, Doppler, azimuth and elevation spectrograms. The system is implemented on a Raspberry Pi 3 B and working in real time. The contributions of the paper are as follows:

- A novel feature extraction algorithm is presented as alternative to conventional range-Doppler processing.
- The competitiveness of the proposed processing compared to conventional FFT based processing is shown on real world data.
- Low complexity of the proposed processing is shown.

2. GESTURE SET AND RADAR SYSTEM DESIGN

The set of gestures used in the paper includes eight macro and two micro gestures. A macro gesture is a motion of the entire hand such as swipe left to right, whereas a micro gesture

is defined by single finger motions such as rubbing with the thumb over the index finger. In Fig. 1 the set of gestures is depicted.

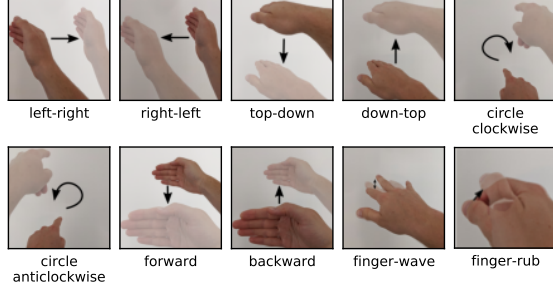


Fig. 1: Set of gestures.

The gesture recognition system presented in the paper uses Infineon’s 60-GHz FMCW radar chipset BGT60TR13C for data acquisition. The radar chipset has one transmit and three receive antennas. The receivers are ordered in a L-shape, which enables an angle estimation on the basis of two antennas each in azimuth as well as elevation direction. The radar is configured to send chirps ranging from $f_{\min} = 58$ GHz to $f_{\max} = 63$ GHz. With a pulse repetition time of $T_{\text{PRT}} = 0.39$ ms the radar sends a burst of 32 chirps. Each received chirp is mixed with the transmit signal. The resulting intermediate frequency signal then undergoes an anti aliasing filter and is sampled 64 times with a frequency of 2 MHz. The signal of such a set of chirps is called data frame and is immediately transferred to the host. The data frames are produced in a frequency of 30 frames/s.

The received and digitized signal is stored in a 4D array $s_0[f, r, n, m]$ with the dimensions $F \times R \times N \times M$, where f is the data frame index, r the receive channel index, n the slow-time index and m the fast-time index. The signal contains undesired DC components, mainly arising from antenna leakage and static objects in the field of view, which have to be removed. Therefore, for each data frame and for each receiving channel the mean is removed along fast-time and along slow-time dimension. The mean removed signal $s[f, r, n, m]$ is the basis for any further processing introduced in this paper.

3. CONVENTIONAL SIGNAL PROCESSING

The frequency of the IF signal depends on the time delay of the received signal and thus is coupled on the range of the back scattering object. Thus, conventionally a FFT along each chirp is applied to obtain the range information within the signal. Motion of the back scattering object result in a change of phase within the corresponding fast-time frequency or range bin introducing the Doppler shift. Since the phase is periodic, the frequency within a range bin across multiple chirps indicates the radial speed of the target.

Range and Doppler spectrograms: To obtain a real valued signal, the amplitude of the RDIs is used in this processing step. Since only a single target within the field of view can be assumed in short range gesture sensing the 2D RDIs can be marginalized in both dimensions to get a range and a Doppler vector, without losing much information about the object of interest, whereas the data dimension can be reduced. The range and Doppler vectors of consecutive frames are concatenated and form a 2D range or Doppler spectrogram respectively. The range and Doppler spectrograms of the three receiving channels are finally integrated to increase the signal-to-noise ratio (SNR).

Angle spectrogram: The angle of arrival is estimated based on the range-Doppler bin with the highest amplitude in the RDI. Based on the complex value of the range-Doppler bin found by a peak search on the amplitudes a digital beamforming expressed as

$$a(\hat{\theta}) = \sum_{r \in R} x_r \exp\left(-j \frac{2\pi d^r \sin(\hat{\theta})}{\lambda}\right) \quad (1)$$

is applied. In (1) R is the set of receiving channels across which the digital beamforming should be applied, x_r is the complex valued selected range-Doppler bin of the r^{th} channel and $\hat{\theta}$ is the estimated angle swept across the field of view at predefined angular steps. For azimuth angle estimation R is the set of antenna 1 and 3 and for elevation angle estimation R is the set of antenna 2 and 3. Exemplary images of a set of range, Doppler, azimuth and elevation spectrograms are depicted in Fig. 2.

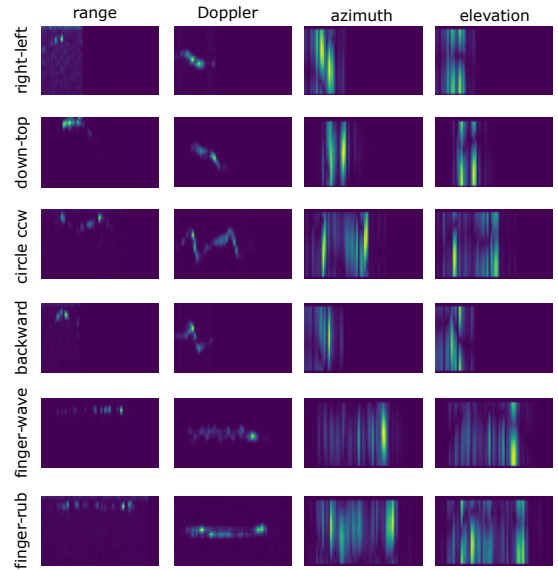


Fig. 2: Exemplary set of spectrograms for selected gestures. The x-axis of the spectrograms is the time dimension going from 0 to 2 s.

4. PROPOSED TIME SERIES PROCESSING

The used radar chipset provides a real valued signal. To obtain the motion and angle information the phase of the signal is needed. To achieve this, in conventional processing a FFT is applied along fast time. The FFT divides the signal into N range bins with a range resolution of $\frac{c}{2BW}$, where BW is the chirp bandwidth. As also underlined by [2], the fundamental sensing paradigm is not the range profile of the hand, since the range resolution is anyway too coarse, but the analysis of the scattering center dynamics through processing of temporal changes that occur in the raw signal over slow time. Therefore, it is superfluous to resolve the signal in range direction using a FFT, which comes with a high computational complexity. Instead, we propose to apply a complex valued low pass sinc filter to the fast time signal. This has two positive effects: First, the low pass filter acts as a limitation of the field of view, thus masking out all motions outside of the region of interest and second, the signal is transformed to complex domain which allows an easy access to the phase information with high temporal resolution.

For low pass filtering a complex valued 1D sinc filter is used. The filter is defined as

$$h[m, f_c, b] = 2b \operatorname{sinc}(2bt)e^{jmT} \quad (2)$$

with $m \in [-\lfloor \frac{M}{2} \rfloor, \lfloor \frac{M}{2} \rfloor]$, where M is the filter length, T the sampling interval, f_c the center frequency and b the bandwidth. Since the signal is static within a chirp, no convolution per se is performed but the fast time signal is just multiplied by the complex valued sinc filter. Thus, the signal within a data frame after filtering is complex valued and one dimensional. The signal is defined as

$$s[f, r, n] = s[f, r, n, m] \cdot h[m, f_c, b] \cdot w[m] \quad (3)$$

where $w[m]$ is a window function. Further, f_c is chosen to be 0.25 normalized frequency and b is set to 0.5 normalized frequency. The resulting complex valued signal is stored as magnitude $m[f, r, n] = |s[f, r, n]|$ and phase $\phi[f, r, n] = \arg(s[f, r, n])$.

Magnitude: The magnitude array is flattened by concatenating the signal of multiple frames followed by an integration over all receiving channels. As a result the array holding the magnitude of the signal is simply defined as $m[k]$, where k ranges from 0 to $F \times N$.

Azimuth and elevation angle: To extract information about the angle of arrival the phase difference between two antennas r_0 and r_1 is used as defined in (4).

$$\Delta\phi_{r_0, r_1}[f, n] = \phi[f, r_0, n] - \phi[f, r_1, n] \quad (4)$$

The relation between phase difference in spatial dimension and the angle of arrival in the 1D case can be expressed as $\theta = \sin^{-1}(\frac{\lambda\Delta\phi}{2\pi d})$ where λ is the wavelength and d the antenna distance. For the used radar the antenna distance d is

half a wavelength. Given this fact, the relation between phase offset and angle of arrival can be approximated to be linear. Thus, for simplicity we directly interpret the phase difference as angle of arrival.

Also the phase difference signal is flattened over the frames similar as it was done for the magnitude signals. Thus, the phase difference signal becomes the 1D array $\Delta\theta_{r_0, r_1}[k]$. To increase the SNR the spatial phase difference is accumulated. Therefore, the resulting signal representing information about the angle of arrival is defined as

$$\text{aoa}_{r_0, r_1}[k] = \sum_i^k \Delta\phi_{r_0, r_1}[i]. \quad (5)$$

Note that due to integration the steepness of the signal represents the angle of arrival. The array containing information about the azimuth angle is defined by choosing antenna 1 and 3 as r_0 and r_1 whereas the elevation angle is estimated between antenna 2 and 3. Therefore, the azimuth array is defined as $\text{az}[k] = \text{aoa}_{1,3}[k]$ and the elevation array is defined as $\text{el}[k] = \text{aoa}_{1,2}[k]$.

Relative range: By phase unwrapping in slow time direction the relative range can be estimated. However, the idle time between data frames cause a random phase offset between first sampling point in the current frame and the last sample in the previous frame. Therefore, simply concatenating the frames and then evaluating the phase displacement would lead to discontinuities between the frames. Instead the phase difference in slow time direction is first estimated within each frame $\Delta\phi[f, r, n] = \phi[f, r, n+1] - \phi[f, r, n]$. Then the phase difference signals are concatenated over frame dimension. Due to the difference the resulting signal is F data points smaller than the magnitude and angle arrays. Thus between the frames a phase difference is approximated by a linear interpolation between the last and first phase difference of two consecutive frames as defined in (4). The resulting signal is then integrated over the receiving channels, which finally leads to another 1D signal of size $F \times N$ describing the targets relative radial position over time.

Thus, in total the radar signal of a recorded gesture is represented as four 1D time series' namely the relative range, the integrated azimuth phase offset, the integrated elevation phase offset and the absolute value. An illustrative example of a set of range, azimuth, elevation and absolute value time series for each gesture is plotted in Fig. 3. Despite the idle time between the frames the 1D time series data is smooth and without discontinuities. Thus, it can be nicely processed by a 1D CNN without causing artifacts in the convolution.

5. EXPERIMENT AND RESULTS

In the first part of this section the classification accuracy of two similar ConvNets trained by conventional spectrograms and the proposed time series data, respectively, is compared,

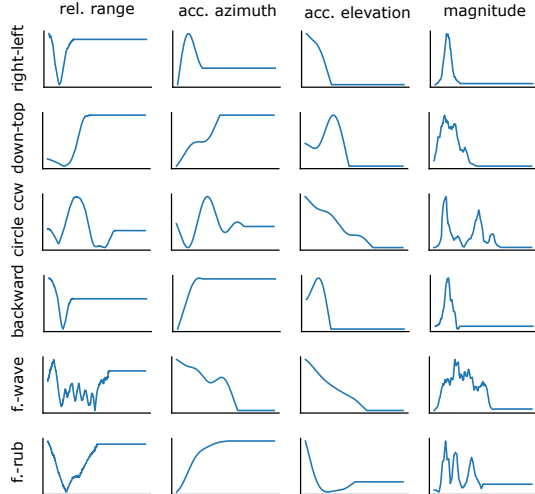


Fig. 3: Exemplary set of time series for selected gestures. The x-axis of the plots is the time dimension going from 0 to 2 s.

whereas the second part discusses the computational complexity of both systems. The used dataset consists of the 10 gestures introduced in sec. 2. In total 300 repetitions per gesture were recorded from 8 different people. The train and test dataset were split by person. Thus, 250 samples from 6 persons for each class is used for training and 50 samples from 2 different persons per class is used for testing. Further, each training is repeated 10 times to reduce the variance in the results.

5.1. Classification Accuracy

For time series classification a 3 layered 1D CNN is used. The first convolutional layer uses 32 filters with a kernel size of 64, the second and third layer are using 32 kernels with a filter width of 16. As very first input layer a average pooling of size 4 is used and after each convolutional layer an max-pooling of size 2 is performed and a rectified linear unit (ReLU) is applied as activation function. After the convolutional block the tensor is flattened and fed into a fully connected layer with 32 output dimensions followed by a fully connected layer with 10 output dimensions and softmax activation. The neural network processing the set of spectrograms is 3 layered 2D CNN with 32, 64 and 64 filters of the sizes 5x5, 3x3 and 3x3. Max pooling is used after each convolutional layer and a ReLU is used as activation. Also here the convolutional block is followed by a fully connected layer with 32 outputs and a fully connected layer with 10 outputs and softmax activation.

Cross entropy is used as loss function and stochastic gradient descent with a learning rate of 0.005 is used as optimizer for both models. The trainings are carried out 10 times and the mean accuracy as well as the standard deviation is used as metric. The classification results along with the number of parameters and the number of mega floating point opera-

tions (MFLOPs) needed for one prediction are given in Tab. 1. Both models achieve a similar accuracy of about 96%.

5.2. Computational Complexity

Processing a data frame of size $N \times M$ by a FFT comes with a computational complexity of $\mathcal{O}(NM \log(NM))$. With the proposed processing the 2D FFT is replaced by a multiplication of each chirp with a single complex valued sinc filter which has a complexity of $\mathcal{O}(NM)$. Creating the range, azimuth, elevation and magnitude signal is done in $\mathcal{O}(N)$. Thus, the computational complexity of processing a data frame was reduced from $\mathcal{O}(NM \log(NM))$ to only $\mathcal{O}(NM)$. It is noteworthy that with FFT processing the target angle has to be additionally estimated, whereas the angle information is already extracted in the proposed processing.

Although the ConvNet interpreting the time series data is only one dimensional, it has more parameters than the 2D ConvNet. The reason is that the system has to interpret time series data. Therefore, there are no clear edges as in the image like 2D spectrogram representation. Thus, we are using larger filter sizes to cover a larger receptive field. However, the 1D ConvNet has less than half the MFLOPs to perform compared to the 2D ConvNet doing a single prediction. Thus the hardware requirements are significantly reduced by maintaining the same classification accuracy.

In order to demonstrate the functionality and real-time capability of the system under limited hardware resources, the system was run on a Raspberry Pi 3 B. Neither the preprocessing nor the neural network were optimized. Nevertheless, the preprocessing takes about 100 ms and predicting a class takes about 50 ms resulting in a reaction time of only 150 ms in total.

Table 1: Comparison of 2D ConvNet using 2D preprocessed spectrograms and 1D ConvNet using the 1D time series as input with respect to classification accuracy, memory footprint and computational complexity.

Model	Acc. (\pm dev.)	# parameter	MFLOPs
2D ConvNet (spectrograms)	95.7% (\pm 0.9%)	51488	8.960
1D ConvNet (time series)	96.0% (\pm 0.8%)	70784	3.719

6. CONCLUSION

In this paper a promising alternative to the dominating FFT based preprocessing for FMCW radars was proposed. The proposed processing reduces the computational complexity for preprocessing a single data frame to $\mathcal{O}(NM)$. It was experimentally shown on real world data that the novel processing is capable of achieving comparable classification performance to conventional FFT preprocessed data.

7. REFERENCES

- [1] Avik Santra and Souvik Hazra, *Deep learning applications of short-range radars*, Artech House, 2020.
- [2] Jaime Lien, Nicholas Gillian, M Emre Karagozler, Patrick Amihood, Carsten Schwesig, Erik Olson, Hakim Raja, and Ivan Poupyrev, “Soli: Ubiquitous gesture sensing with millimeter wave radar,” *ACM Transactions on Graphics (TOG)*, vol. 35, no. 4, pp. 1–19, 2016.
- [3] Yong Wang, Aihu Ren, Mu Zhou, Wen Wang, and Xiaobo Yang, “A novel detection and recognition method for continuous hand gesture using fmcw radar,” *IEEE Access*, vol. 8, pp. 167264–167275, 2020.
- [4] Myoungseok Yu, Narae Kim, Yunho Jung, and Seongjoo Lee, “A frame detection method for real-time hand gesture recognition systems using cw-radar,” *Sensors*, vol. 20, no. 8, 2020.
- [5] Jae-Woo Choi, Si-Jung Ryu, and Jong-Hwan Kim, “Short-range radar based real-time hand gesture recognition using lstm encoder,” *IEEE Access*, vol. 7, pp. 33610–33618, 2019.
- [6] Souvik Hazra and Avik Santra, “Robust gesture recognition using millimetric-wave radar system,” *IEEE Sensors Letters*, vol. 2, no. 4, pp. 1–4, 2018.
- [7] Matthias G. Ehrnsperger, Thomas Brenner, Henri L. Hoese, Uwe Siart, and Thomas F. Eibert, “Real-time gesture detection based on machine learning classification of continuous wave radar signals,” *IEEE Sensors Journal*, vol. 21, no. 6, pp. 8310–8322, 2021.
- [8] Wentai Lei, Xinyue Jiang, Long Xu, Jiabin Luo, Mengdi Xu, and Feifei Hou, “Continuous gesture recognition based on time sequence fusion using mimo radar sensor and deep learning,” *Electronics*, vol. 9, no. 5, 2020.
- [9] Davi Rodrigues and Changzhi Li, “Hand gesture recognition using fmcw radar in multi-person scenario,” in *2021 IEEE Topical Conference on Wireless Sensors and Sensor Networks (WiSNeT)*, 2021, pp. 50–52.
- [10] Eiji Hayashi, Jaime Lien, Nicholas Gillian, Leonardo Giusti, Dave Weber, Jin Yamanaka, Lauren Bedal, and Ivan Poupyrev, “Radarnet: Efficient gesture recognition technique utilizing a miniature radar sensor,” in *Proceedings of the 2021 CHI Conference on Human Factors in Computing Systems*, New York, NY, USA, 2021, CHI ’21, Association for Computing Machinery.
- [11] Mateusz Chmurski, Mariusz Zubert, Kay Bierzynski, and Avik Santra, “Analysis of edge-optimized deep learning classifiers for radar-based gesture recognition,” *IEEE Access*, vol. 9, pp. 74406–74421, 2021.
- [12] Yuliang Sun, Tai Fei, Xibo Li, Alexander Warnecke, Ernst Warsitz, and Nils Pohl, “Real-time radar-based gesture detection and recognition built in an edge-computing platform,” *IEEE Sensors Journal*, vol. 20, no. 18, pp. 10706–10716, 2020.
- [13] Moritz Scherer, Michele Magno, Jonas Erb, Philipp Mayer, Manuel Eggimann, and Luca Benini, “Tinyradarnn: Combining spatial and temporal convolutional neural networks for embedded gesture recognition with short range radars,” *IEEE Internet of Things Journal*, pp. 1–1, 2021.